Supporting Information for *Environmental Science: Nano*

Ultrathin Graphene Oxide Membrane with Constructed Tent-shaped Structures for Efficient and Tunable Molecular Sieving

Kaijie Yang [1, 2], Tingting Pan[1, 2], Seunghyun Hong[2, 3], Kun Zhang[1], Xiaoying Zhu [1], Baoliang Chen[1*]

1. Department of Environmental Science, Zhejiang University, Hangzhou 310058, China;
2. Advanced Membranes and Porous Materials (AMPM) Center, Physical Sciences and Engineering Division, King Abdullah University of Science and Technology, Thuwal, Jeddah 23955-6900, Saudi Arabia
3. Materials Science and Engineering, Physical Sciences and Engineering Division, King Abdullah University of Science and Technology, Thuwal 23955-6900, Saudi Arabia

*Corresponding Author Email: blchen@zju.edu.cn

Supporting information consists of 26 pages, including this one.

There are 22 Figures.

Detailed process for GO fabrication

GO layers were synthesized from natural graphite flakes through the modified Hummers method. The detailed procedures are described as follows. Pristine graphite was firstly pre-oxidized. 10 g graphite flakes were added into 30 ml concentrated H_2SO_4 containing 8.33 g $K_2S_2O_8$ and 8.33 g P_2O_5. After reaction at 80 ºC for 4.5 h, the products were collected and washed until the pH became neutral. The pre-oxidized graphite was then dried at 60 ºC.

The following oxidation was processed as the followings. 5 g $NaNO_3$ and 30 g $KMnO_4$ were firstly dispersed into 230 ml pre-cooled H_2SO_4 (temperature < 4 ºC). Then 10 g pre-oxidized graphite was followingly added. After oxidation for 2 h, 460 mL of deionized water was slowly added to heat the mixture and increase the oxidation level. Then 22 mL H_2O_2 was added for further oxidation. The solid products were collected and washed by 10% HCl to remove the residual SO_4^{2-} and metal ions. Then the obtained products were ultrasonicated to exfoliate and collected by centrifugation. The ultrasonication and centrifugation steps were repeated 3 times to completely exfoliate the graphene layers. To purify the products, the final GO dispersion was subjected to dialysis until it reached pH 7.

The detailed process of characterization

The morphology and size of GO were characterized by AFM (Dimension Icon, Bruker). 1 mg/L GO dispersion was dropped on mica plate and dried at 25℃.

The elemental content of GO was analyzed combining EDS and C, H, N element analysis.

The morphology and diameter of SiO_2 were characterized by FE-SEM (SU-8010, Hitachi Co.). 1 mg/L SiO_2 dispersion was dropped on aluminum plate, dried at 25℃ and spayed by gold.

The surface functional groups of GO layers and SiO_2 nanospheres were detected by FTIR (Nicolet 6700, Thermo Scientific) in the 4000-400 cm^{-1} region.

The Zeta potential variation of GO layers and SiO_2 nanospheres according to pH were detected by a surface potentiometer (Zetasizer Nano ZS, Malvern). During the evaluation, the concentrations of GO and SiO_2 were controlled at 40 mg/L and 2 mg/ml and the final equal pH were manipulated by the addition of HCl and $NH_3 \cdot H_2O$.

Membranes' surface and cross-section structures were observed under FE-SEM (SU-8010, Hitachi Co.). For cross-section observation, membranes were wetting-off in liquid nitrogen. Samples were located on an aluminum plate and sprayed by gold to maintain their conductivity.

The interlayer structures of the prepared membrane were characterized by X-ray diffractometer (XRD-7000, Shimadzu Co.) with a copper source. Due to the weak reflection of the ultrathin membrane, thicker membranes (thickness around 5 μm) were applied to enhance the signature. The incident 2 theta angle was started from 5° and ended at 50°.

Membrane's surface Zeta potential was characterized by the electrokinetic analyzer (Surpass 3, Anton Paar). Two pieces of the measured membranes with dimensions of 1 × 2 cm were fitted into measure cell facing parallel with a micro slit of 100 μm. The measurements were performed in 1 mmol/L KCl. The pH was adjusted from 2 to 10 by diluted HCl and NaOH solution. 3 runs were performed at each pH value and 4 measurements were conducted for each run. The average of measured values was used to represent the zeta potential at the given pH.

The surface wettability of SGMs was evaluated by water contact angles measurement performed by a goniometer (OSA 200, Ningbo NB Scientific Instruments Co.) using static sessile drop method. During measurement, 5 μL water drop was loaded on the membrane surface. The water contact angle was captured immediately once the water drop touched the surface. The obtained contact angle was measured by true-drop calculate model.

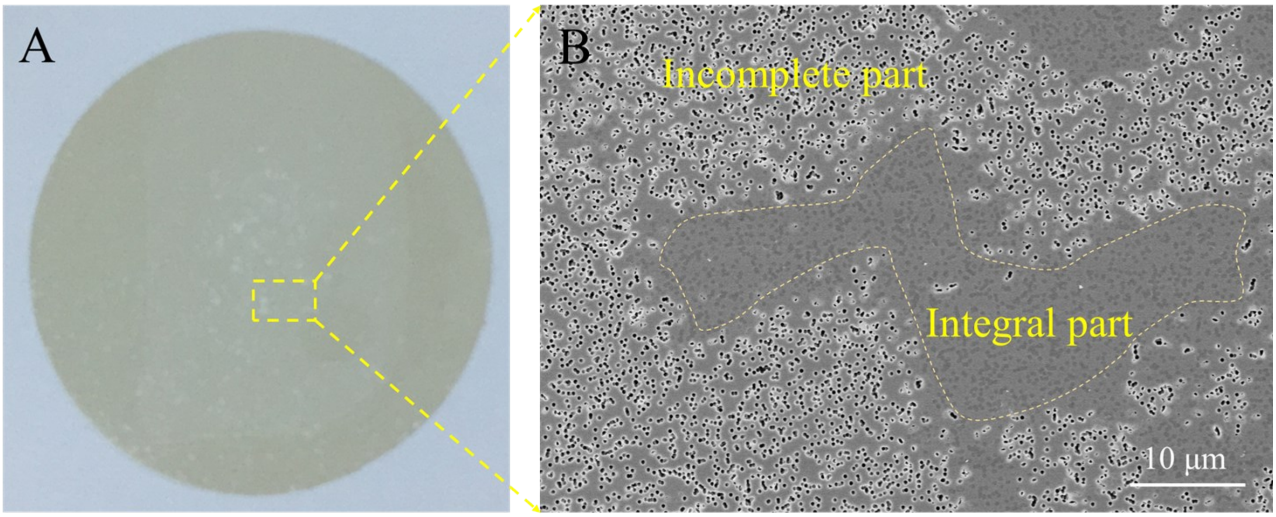

Figure S1. Ultrathin GOM fabricated through traditional filtration assembly. (A) Photo image of GOM fabricated by direct filtration assembly. (B) SEM image of microstructure.

The membrane was fabricated by filtrating 10 ml 3 mg/L GO dispersion through a PC supporting membrane. Characterized by SEM, GOM showed various uncovered defects. These defects were inevitable, even if we changed the glass support or repeated the assembly process. Experimental results showed that it is not reliable to fabricate an integral ultrathin structure using the traditional filtration assembly.

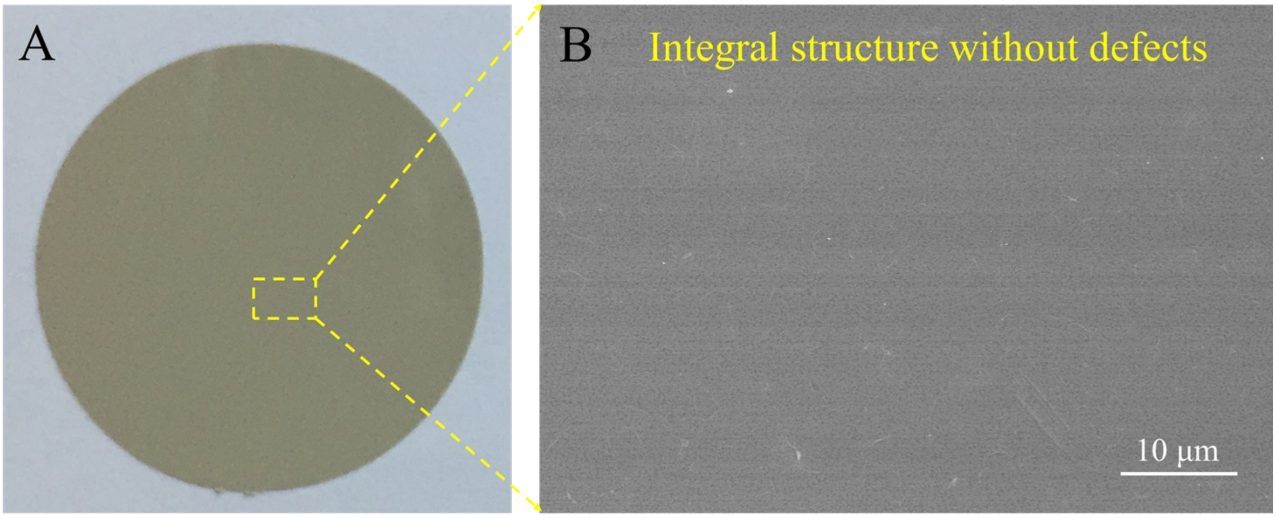

Figure S2. Ultrathin GOM fabricated through the modified method. (A) Photo image of the ultrathin GOM fabricated by the modified method. (B) SEM image of the microstructure.

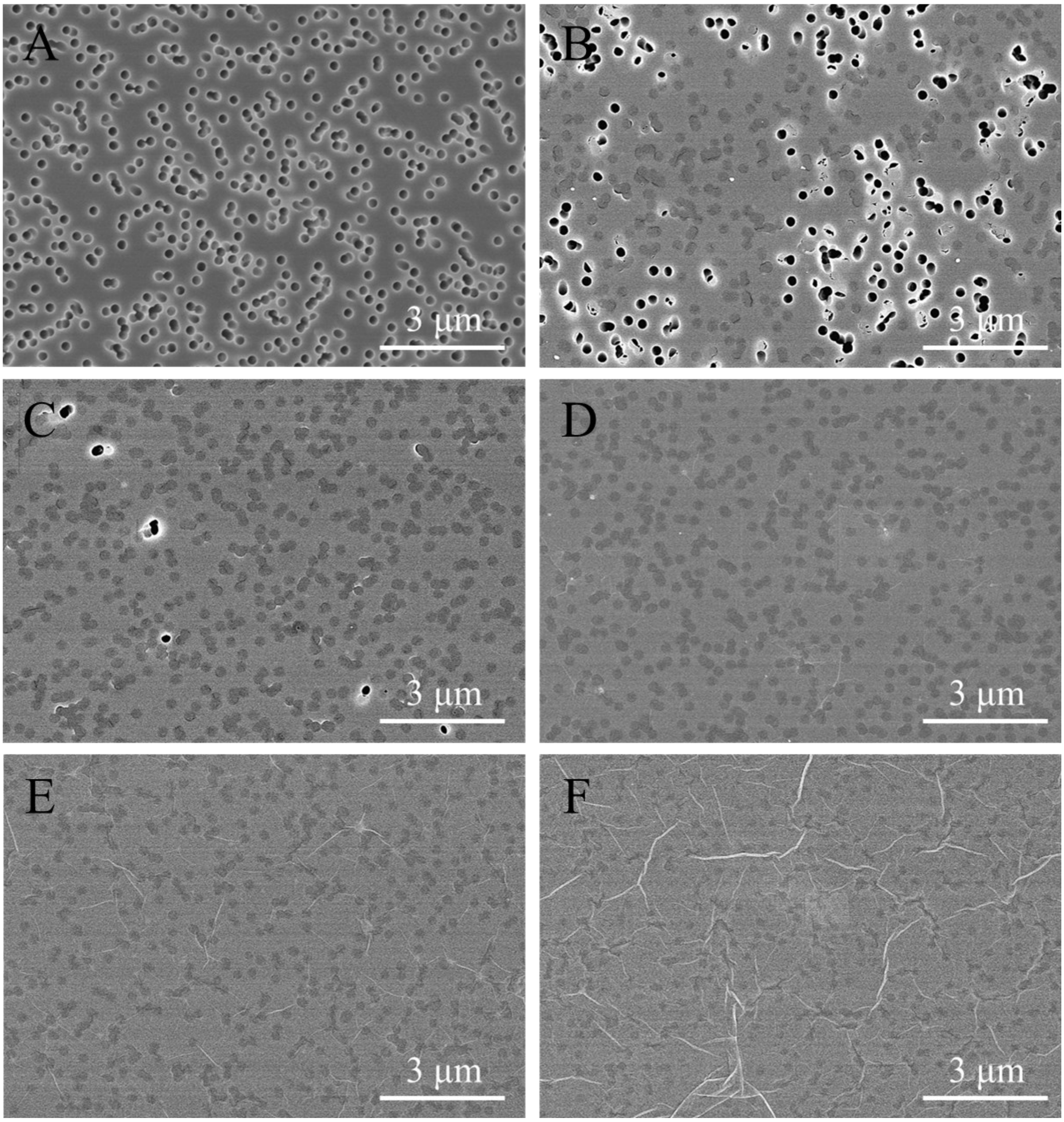

Figure S3. The microstructure of GOMs fabricated with different GO amount. (A) SEM image of pure PS membrane. (B) SEM image of GOM-0.15. (C) SEM image of GOM-0.75. (D) SEM image of GOM-1.5. (E) SEM image of GOM-3. (F) SEM image of GOM-6.

The concentration of filtrated GO dispersion was increased gradually to determine the ultimate thin structure. Pure PC membrane was porous and the diameter of pores was around 0.2 µm. With the increase of added GO, fabricated GOM showed fewer defects. The structure became integral when the concentration of added GO dispersion was higher than 1.5 mg/L.

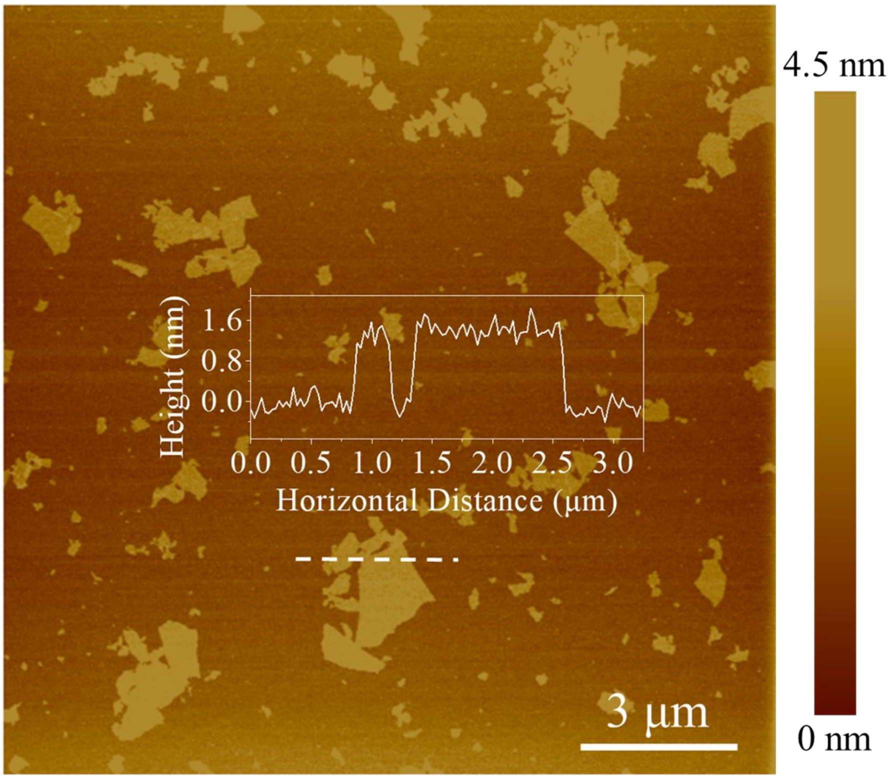

Figure S4. AFM image of GO layers.

As presented in Fig. S4, GO was an ideal two-dimensional layer with a thickness of 1.5 nm. The sizes of GO were various and were mainly distributed in the range of 0.3 - 2 μm.

Table S1. Element content of GO nanosheets

	C (%)	H (%)	O (%)	N (%)	S (%)	Cl (%)
GO	59.76	4.45	34.75	0.071	0.75	0.22

GO's elemental composition was determined by energy dispersive spectrum and elemental analysis. As illustrated in Table S1, except C, GO layers also contained H, O, N, S and Cl. The mass ratio of C, H, O, N, S, Cl was 59.76 wt. %, 4.45 wt. %, 34.75 wt. %, 0.071 wt. %, 0.75 wt. % and 0.22 wt. % respectively.

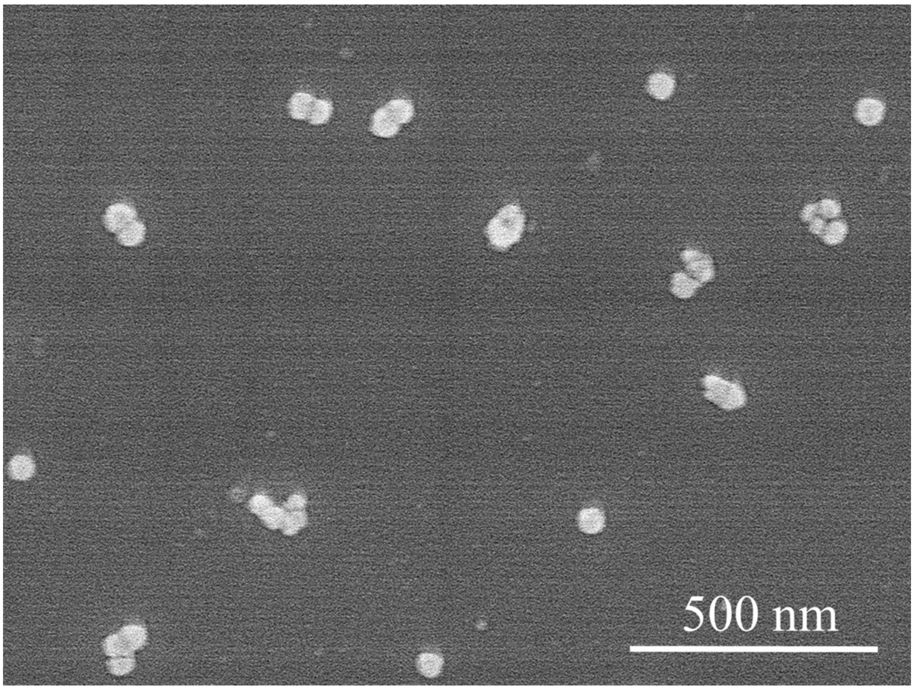

Figure S5. SEM image of SiO_2 nanospheres.

SEM imaging showed SiO_2 nanospheres used in this work had a diameter around 30 nm.

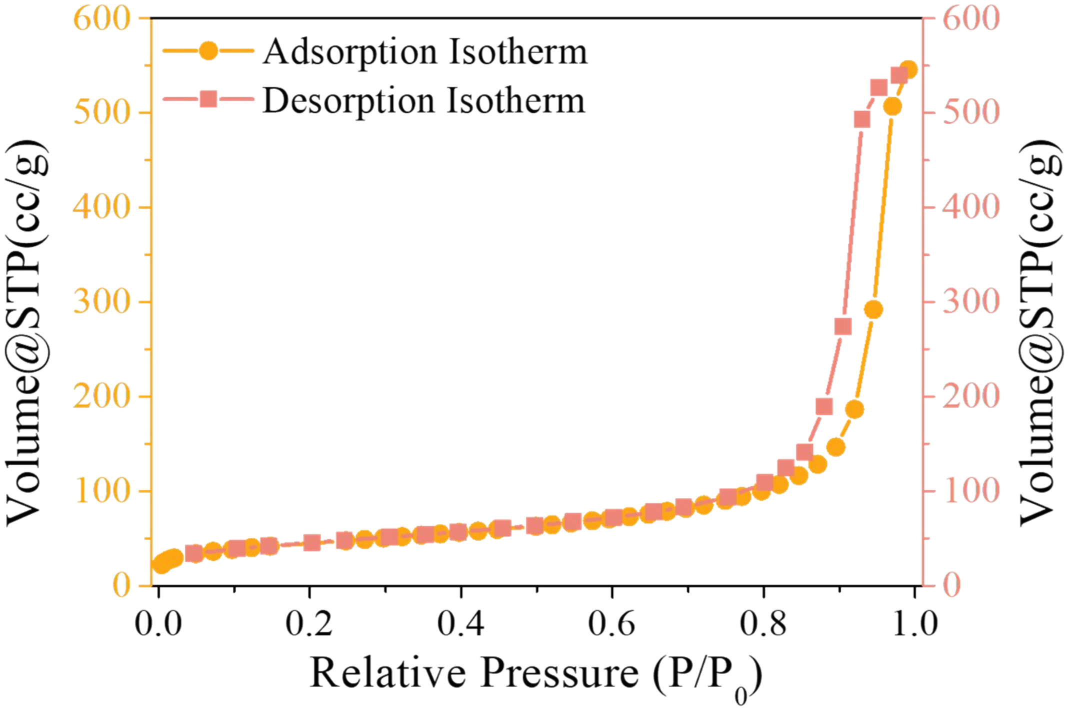

Figure S6. N_2 adsorption and desorption isotherms of SiO_2 nanoparticles.

The surface area of SiO_2 was determined by N_2 adsorption-desorption isotherm. Based on the BET equation, calculated surface area of SiO_2 nanospheres was 156.87 m^2/g.

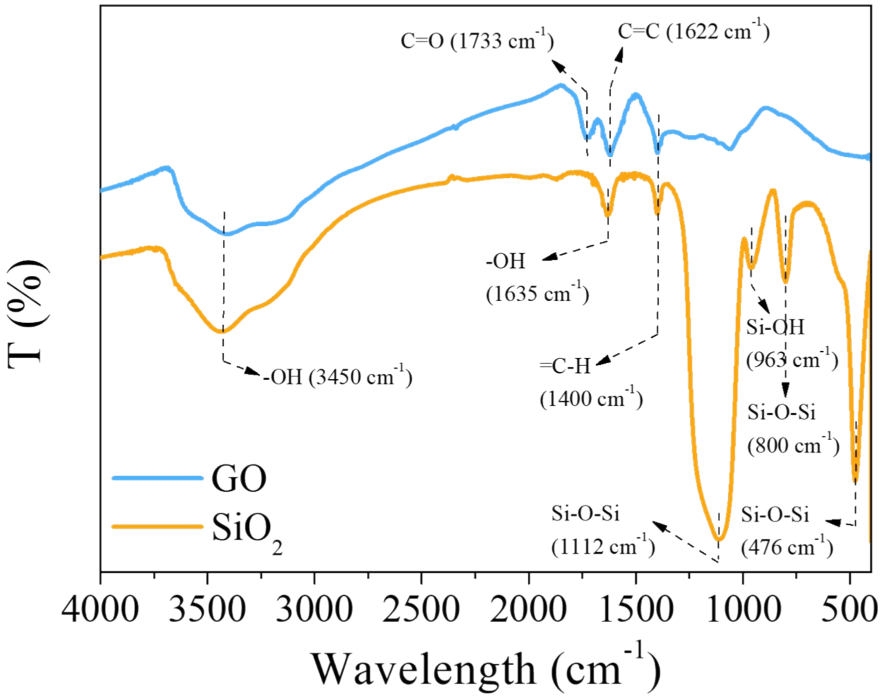

Figure S7. FTIR spectra of GO layer and SiO_2 nanosphere.

The surface functional groups of GO layer and SiO_2 nanosphere were characterized by FTIR spectrum. For SiO_2, the peak at 3450 cm^{-1} and 1635 cm^{-1} presents the bending vibration of –OH of adsorbed water. Peak at 1111 cm^{-1}, 963 cm^{-1}, and 375 cm^{-1} presented the different vibrations of Si-O-Si on SiO_2. Peak at 963 cm^{-1} indicate the stretching vibration of Si-OH. For GO, the peak at 3400, 1735 and 1620 cm^{-1} presented the vibration of –OH, C=O and C=C respectively.

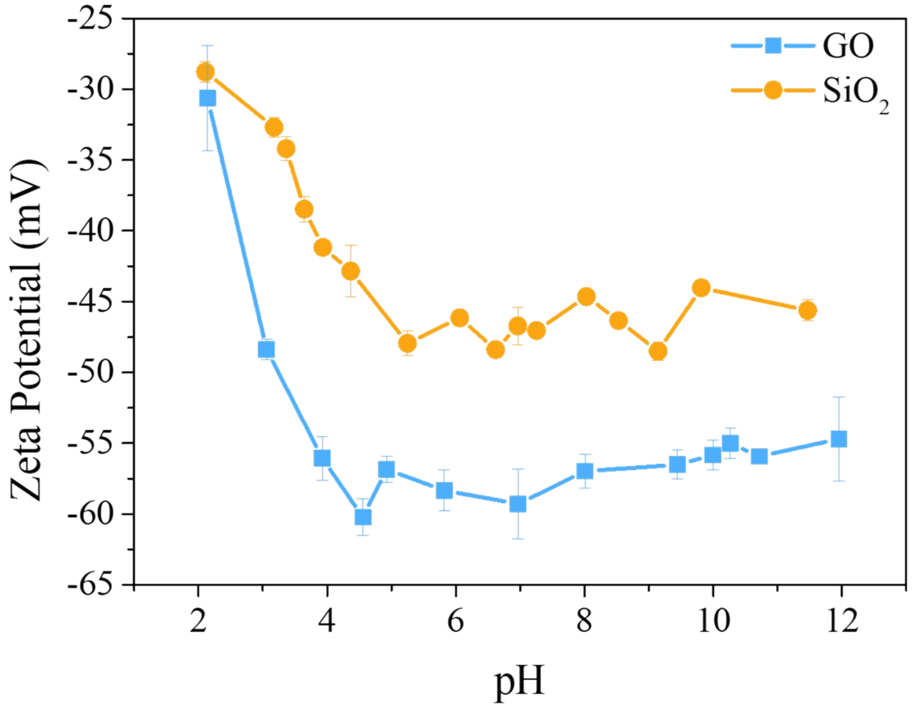

Figure S8. Zeta potential variation of GO layer and SiO_2 nanosphere, according to the pH. Oxygen-containing groups will hydrolyze in water, therefore endow GO layer and SiO_2 nanosphere with the negatively charged surface. The surface electronegativity gradually increased when the pH increased from 2 to 6. Once pH was higher than 6, their zeta potential tended to be steady.

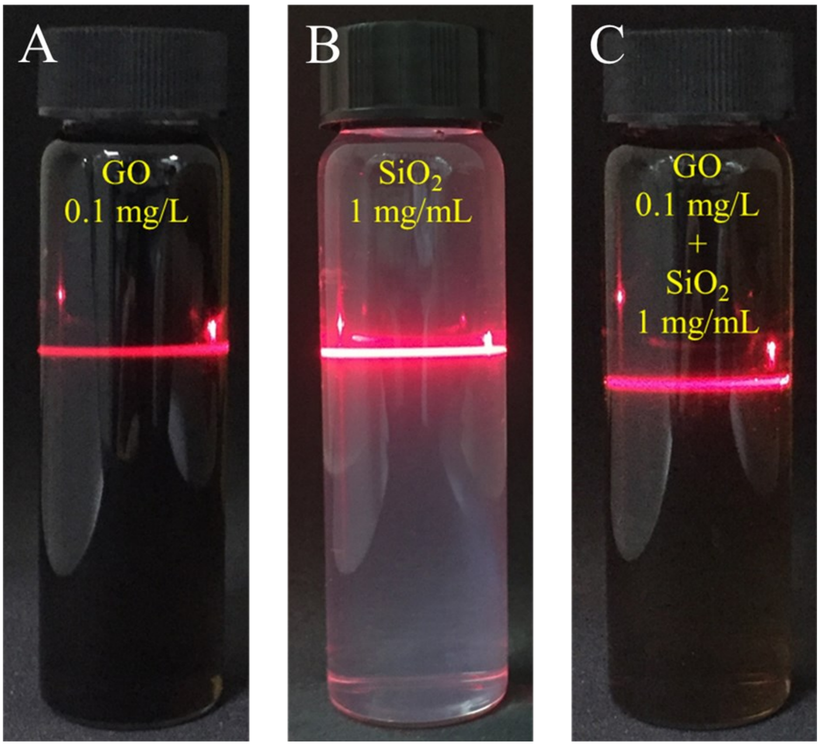

Figure S9. Tyndall effect of dispersions after standing for 1 week. (A) Tyndall effect of GO layer dispersion, (B) Tyndall effect of SiO_2 nanosphere dispersion, (C) Tyndall effect of GO + SiO_2 nanosphere mixture. Dispersions' pH was controlled around 7.

Benefit from the negatively charged surface, GO layer and SiO_2 dispersion can be well dispersed in water. Even after standing for 1 week, dispersions all showed clear Tyndall effect, indicating their good stability.

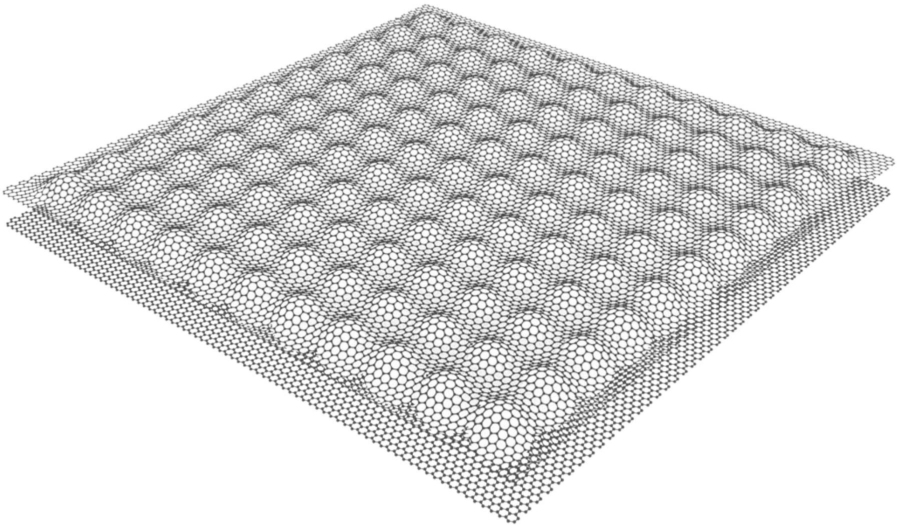

Figure S10. The structural model of GO layer covering on closely arranged SiO_2 nanospheres.

Equation S1. $SA_{GO} = SA_G \times 59.71\%$

Equation S2. $$m_{SiO_2} = \frac{2 \times SA_{GO}}{SA_{SiO_2}}$$

Among the equations, SA_{GO} presents GO's surface area, SA_G presents the theoretical surface area of graphene (2630 m^2/g) and 59.71 % is the mass ratio of C element in GO. Surface area of GO is calculated to be around 1570 m^2/g. m_{SiO_2} presents the maximum weight of SiO_2 nanospheres that 1 g GO layer can cover. SA_{SiO_2} presents the measured surface area of SiO_2 nanospheres (157 m^2/g). According to the calculation, 1 g GO can cover about 20 g SiO_2 nanospheres.

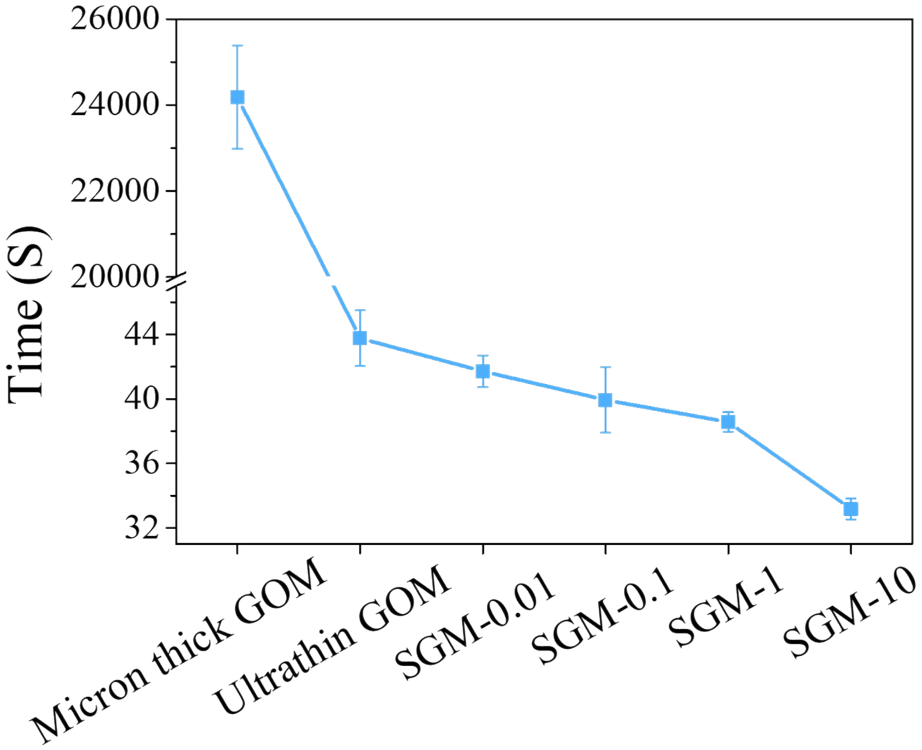

Figure S11. Time-cost of membranes' filtration assembly.

As showed in Fig. S11, micron thick GOM's assembly took around 6 h 40 min. Comparing with the micron thick GOM, ultrathin GOM's assembly was much faster which can be quickly completed within 45 s. With the increasing of SiO_2 intercalating ratio, the assembly was accelerated which took around 42 s for SGM-0.01, 40 s for SGM-0.1, 39 s for SGM-1 and 33 s for SGM-10.

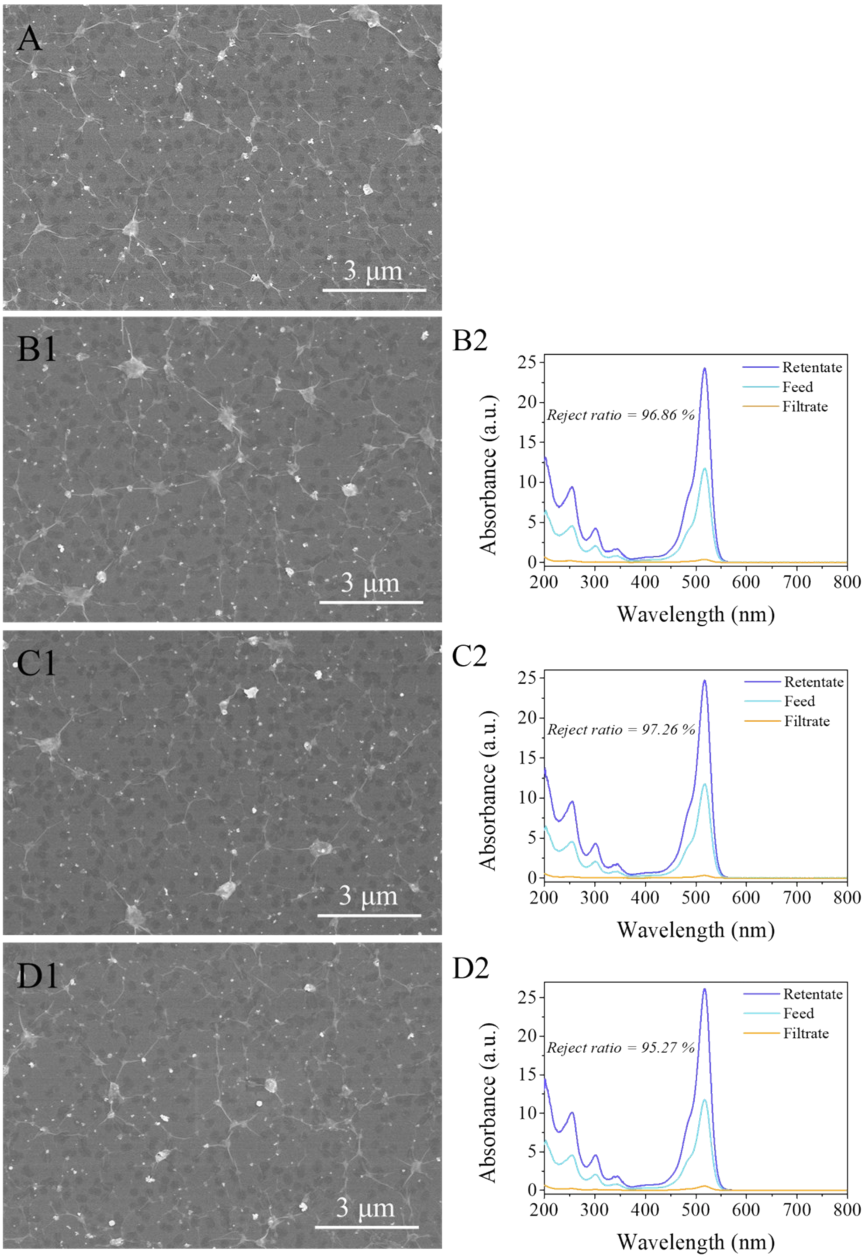

Figure S12. Microstructural characterization and sieving performance evaluation of SGM-0.1 before and after soaking. (A) SEM image of pristine SGM-0.1, (B1) SEM image of SGM-0.1 after immersing in water for 12 h. (B2) Rejection of SGM-0.1 to EY after immersing for 12 h in water. (C1) SEM image of SGM-0.1 after immersing in HCl solution for 12 h. (C2) Rejection of SGM-0.1 to EY after immersing for 12 h in HCl solution. (D1) SEM image of SGM-0.1 after immersing in $NH_3 \cdot H_2O$ solution for 12 h. (D2) Rejection of SGM-0.1 to EY after immersing for 12 h in $NH_3 \cdot H_2O$ solution.

Even after 12 h's shaking, no structural defects were observed under SEM characterization. In addition, EY molecule was selected as a detector for the tiny breaks. Results indicated no decrease of sieving ability happened after immersed in water, HCl solution and $NH_3 \cdot H_2O$.

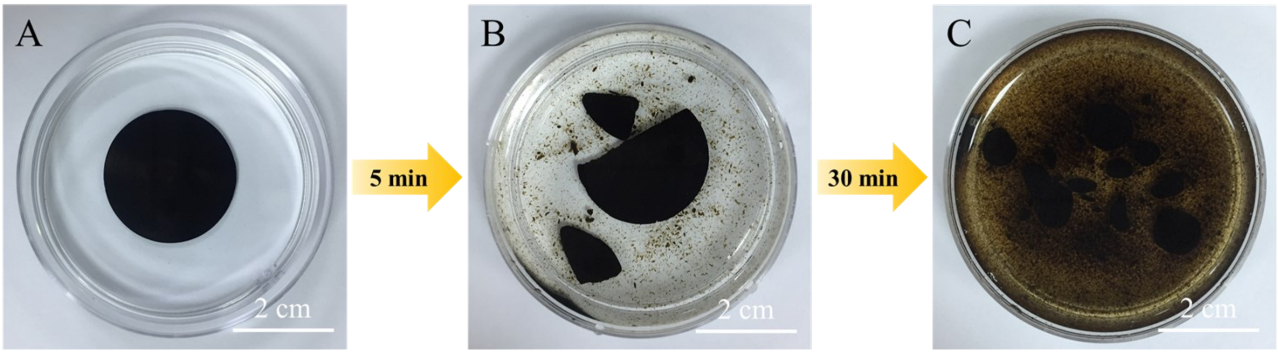

Figure S13. Structural stability evaluation of micron thick GOM in water. (A) Pristine micron thick GOM in water. (B) Micron thick GOM in water after gently shaking 5 min. (C) Micron thick GOM in water after gently shaking 30 min.

Due to the hydrophilic surface and mutual electric repulsion of GO layers, micron thick GOM was unstable in water. After gentle shaking, the membrane structure was disintegrated into parts.

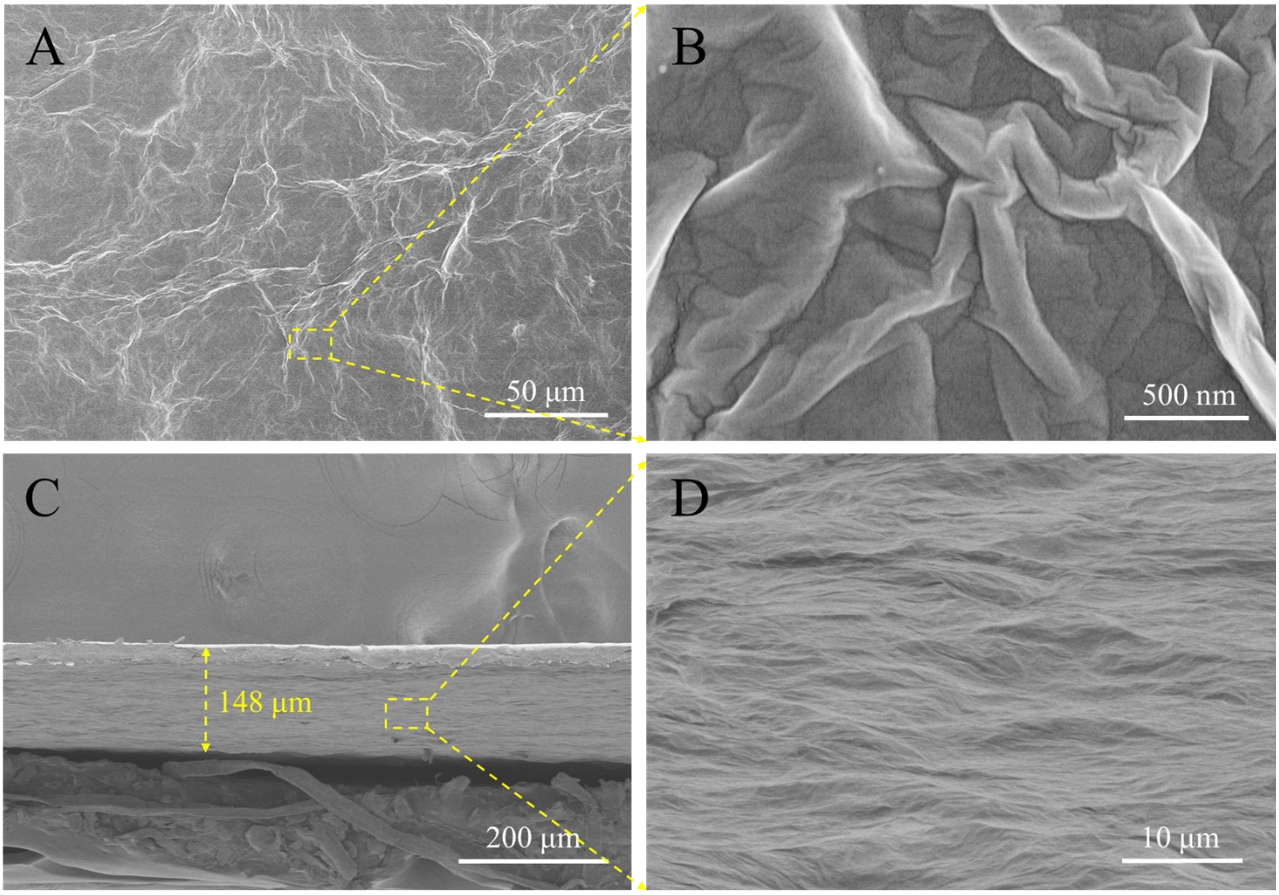

Figure S14. Surface and cross-section structure of micron thick GOM. (A) SEM image of the surface structure of micron thick GOM. (B) Magnified SEM image of the circled area in (A). (C) SEM image of micron thick GOM's cross-section. (D) Magnified image of the circled area in (C).

Micron thick GOM exhibited obvious and large corrugations on the surface because thicker membrane resulted in slower flux and weaker hydraulic shear force. As a result, following assembled layers will deposited with corrugations. Corrugations would weaken the interaction of piled GO layers thereafter resulted in weak stability of GOM. As presented in Fig. S14 C, the thickness of obtained GOM was about 148 μm.

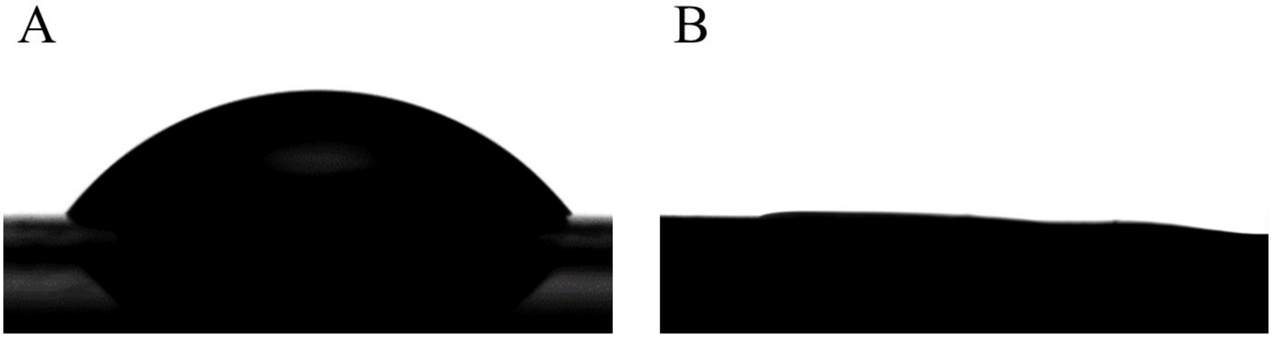

Figure S15. Surface wettability measurement. (A) Waterdrop on GO surface. (B) Waterdrop on SiO_2 surface.

Surface wettability of GO and nano SiO_2 was evaluated by the water contact angle. For the measurements, GO layers were assembled into a macro filter and SiO_2 nanospheres were tiled on glass to form a uniform plane. As presented in Fig. S15, the water contact angle of GOM was 54°. Because of the hydrophilic surface, contacted water would immediately disperse/permeate into SiO_2 plane.

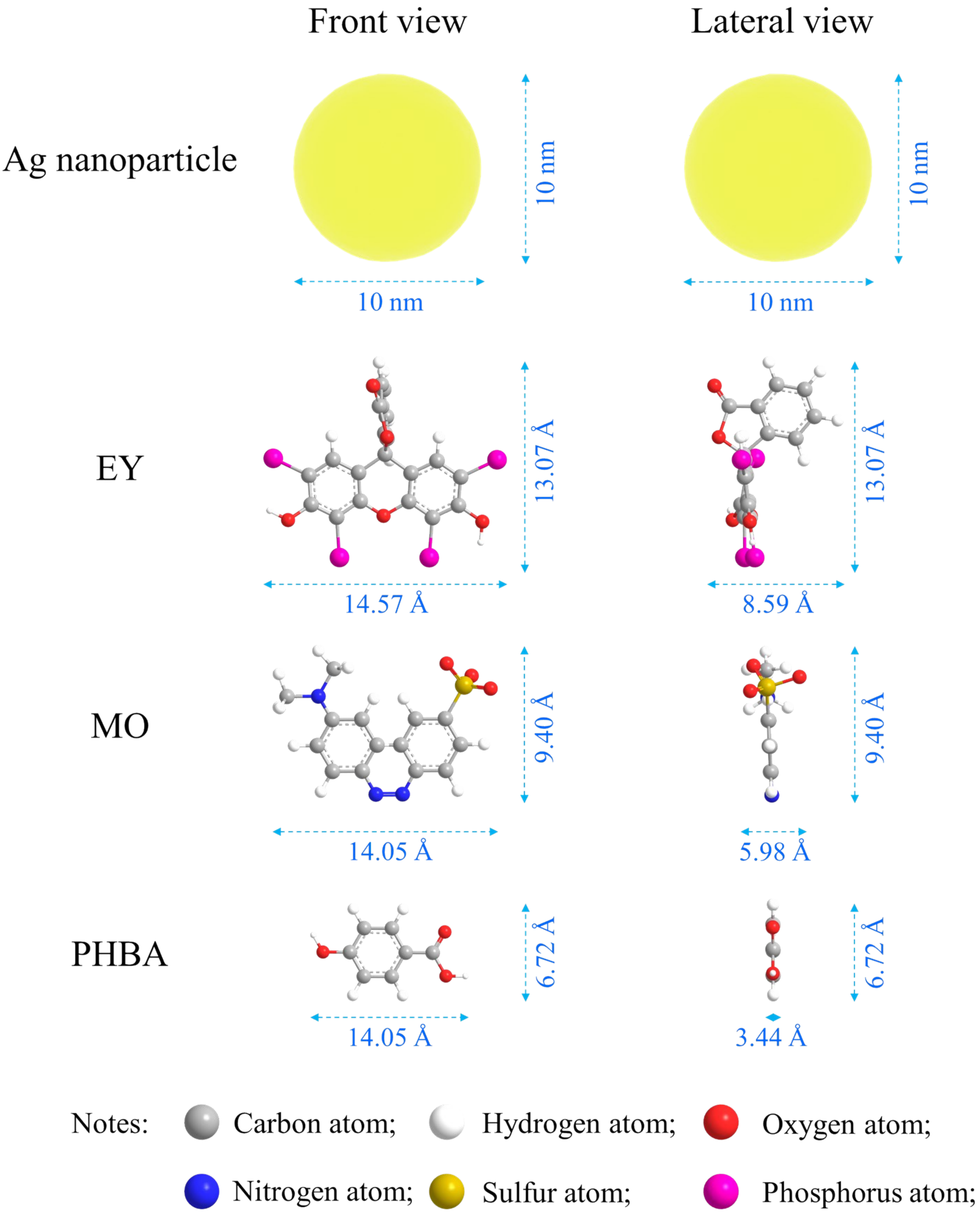

Figure S16. Structure and three-dimensional size of selected nanoparticle and molecules.

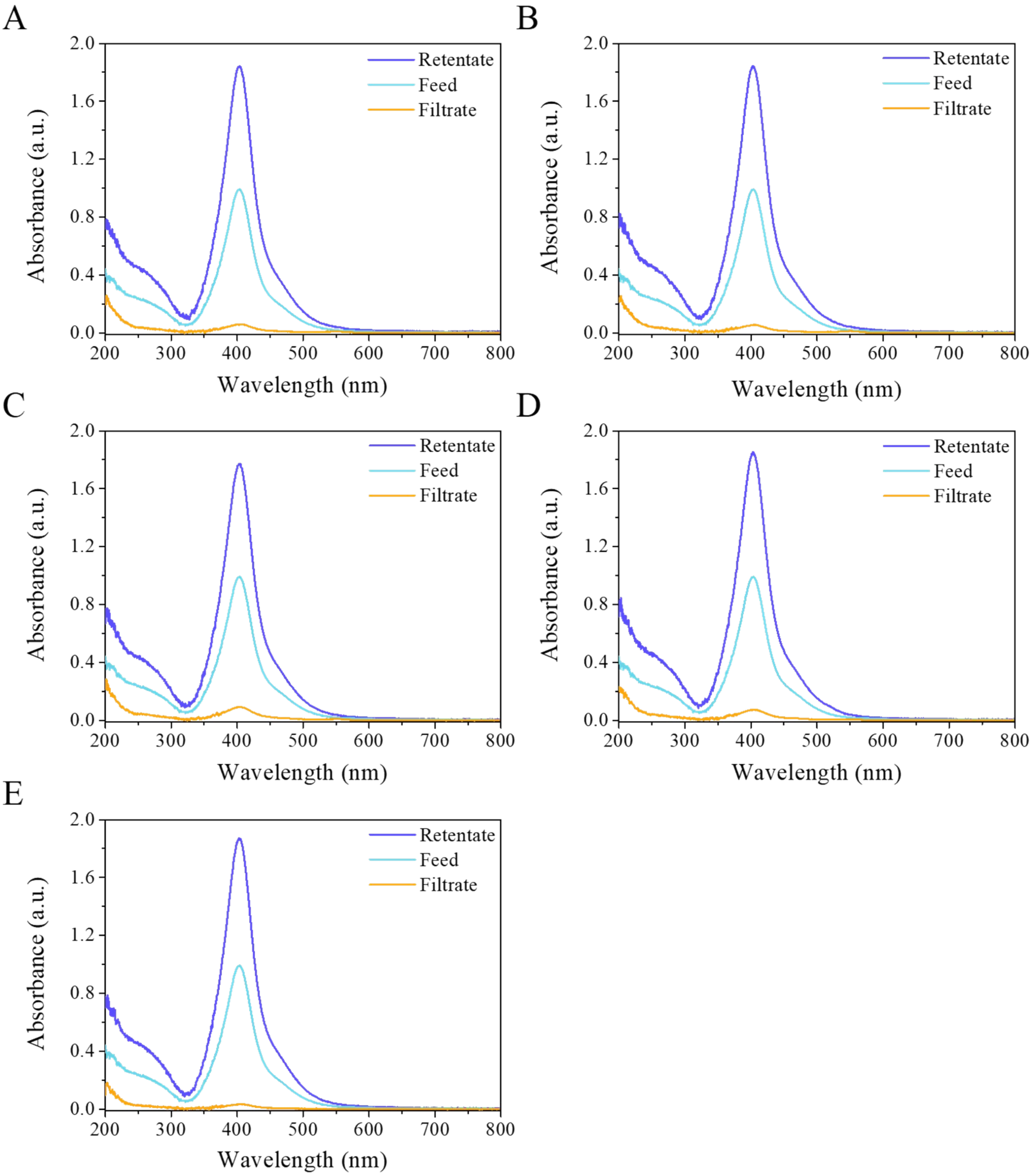

Figure S17. Determination of Ag nanoparticle's concentration in feed, filtrate and retentate, after half of the solution permeated through the membrane. (A) Spectrum of dispersions using GOM as the testing membrane. (B) Spectrum of dispersions using SGM-0.01 as the testing membrane. (C) Spectrum of dispersions using SGM-0.1 as the testing membrane. (D) Spectrum of dispersions using SGM-1 as the testing membrane. (E) Spectrum of dispersions using SGM-10 as the testing membrane.

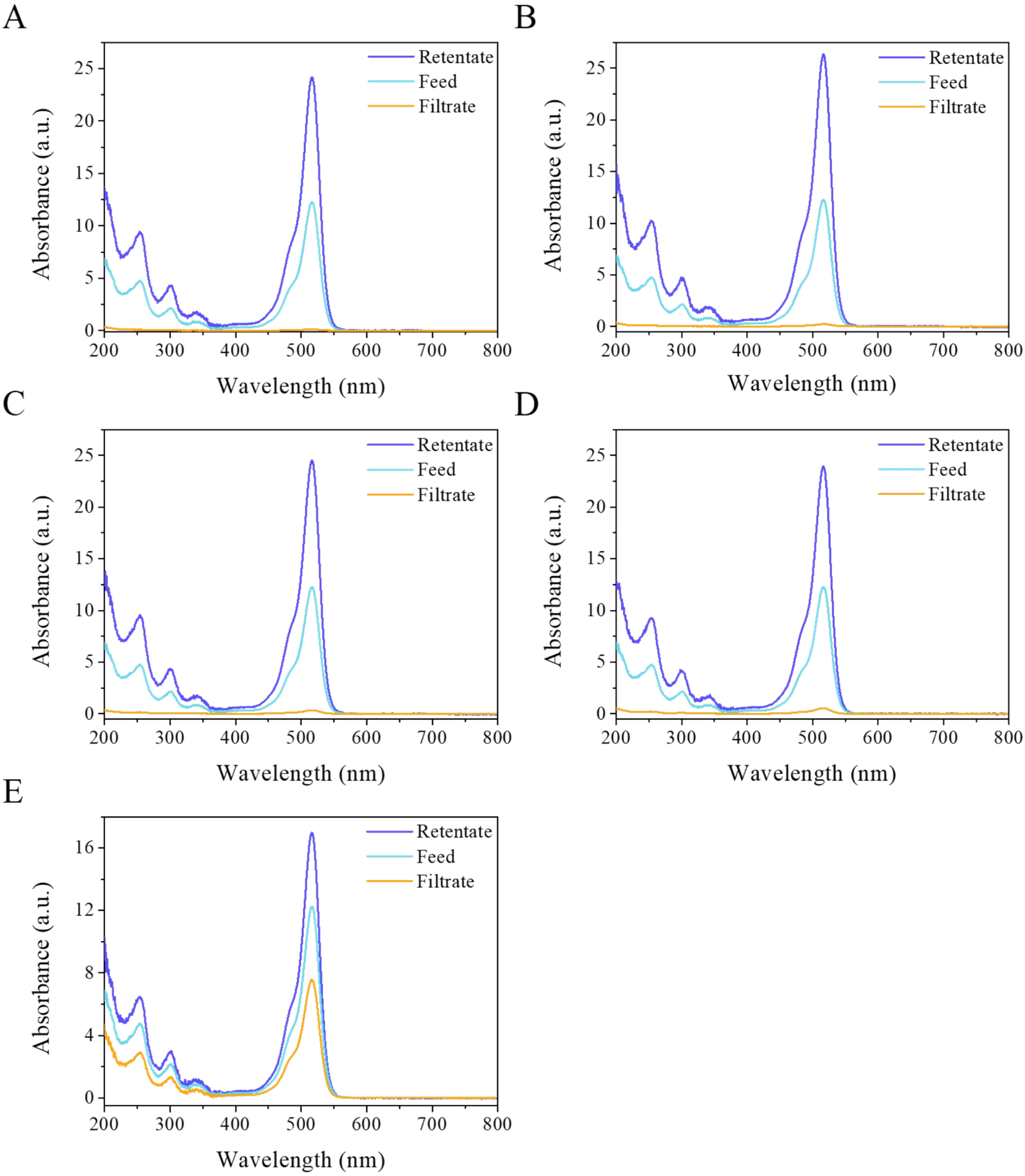

Figure S18. Determination of EY's concentration in feed, filtrate and retentate, after half of the solution permeated through the membrane. (A) Spectrum of solutions using GOM as the testing membrane. (B) Spectrum of solutions using SGM-0.01 as the testing membrane. (C) Spectrum of solutions using SGM-0.1 as the testing membrane. (D) Spectrum of solutions using SGM-1 as the testing membrane. (E) Spectrum of solutions using SGM-10 as the testing membrane.

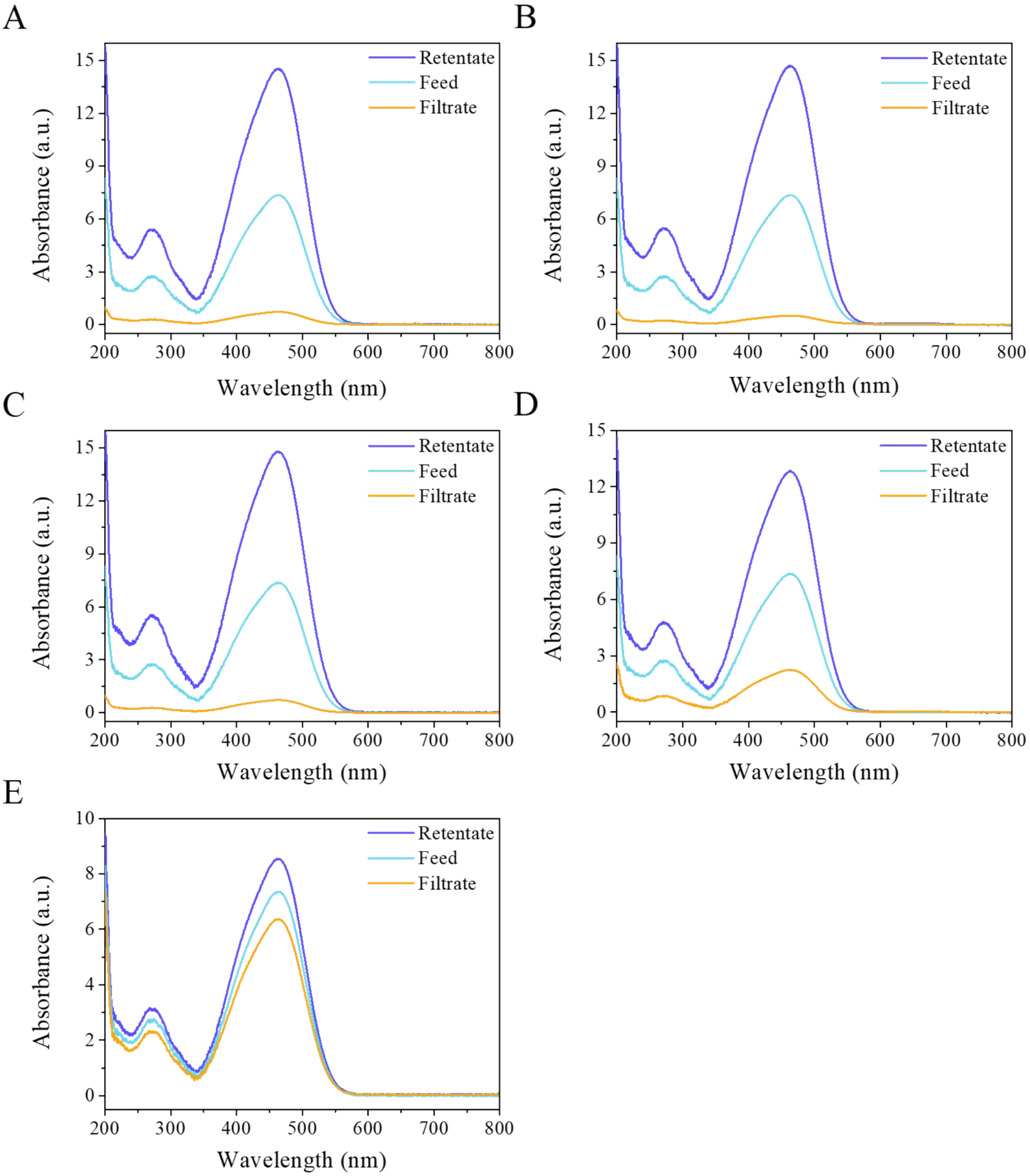

Figure S19. Determination of MO's concentration in feed, filtrate and retentate, after half of the solution permeated through the membrane. (A) Spectrum of solutions using GOM as the testing membrane. (B) Spectrum of solutions using SGM-0.01 as the testing membrane. (C) Spectrum of solutions using SGM-0.1 as the testing membrane. (D) Spectrum of solutions using SGM-1 as the testing membrane. (E) Spectrum of solutions using SGM-10 as the testing membrane.

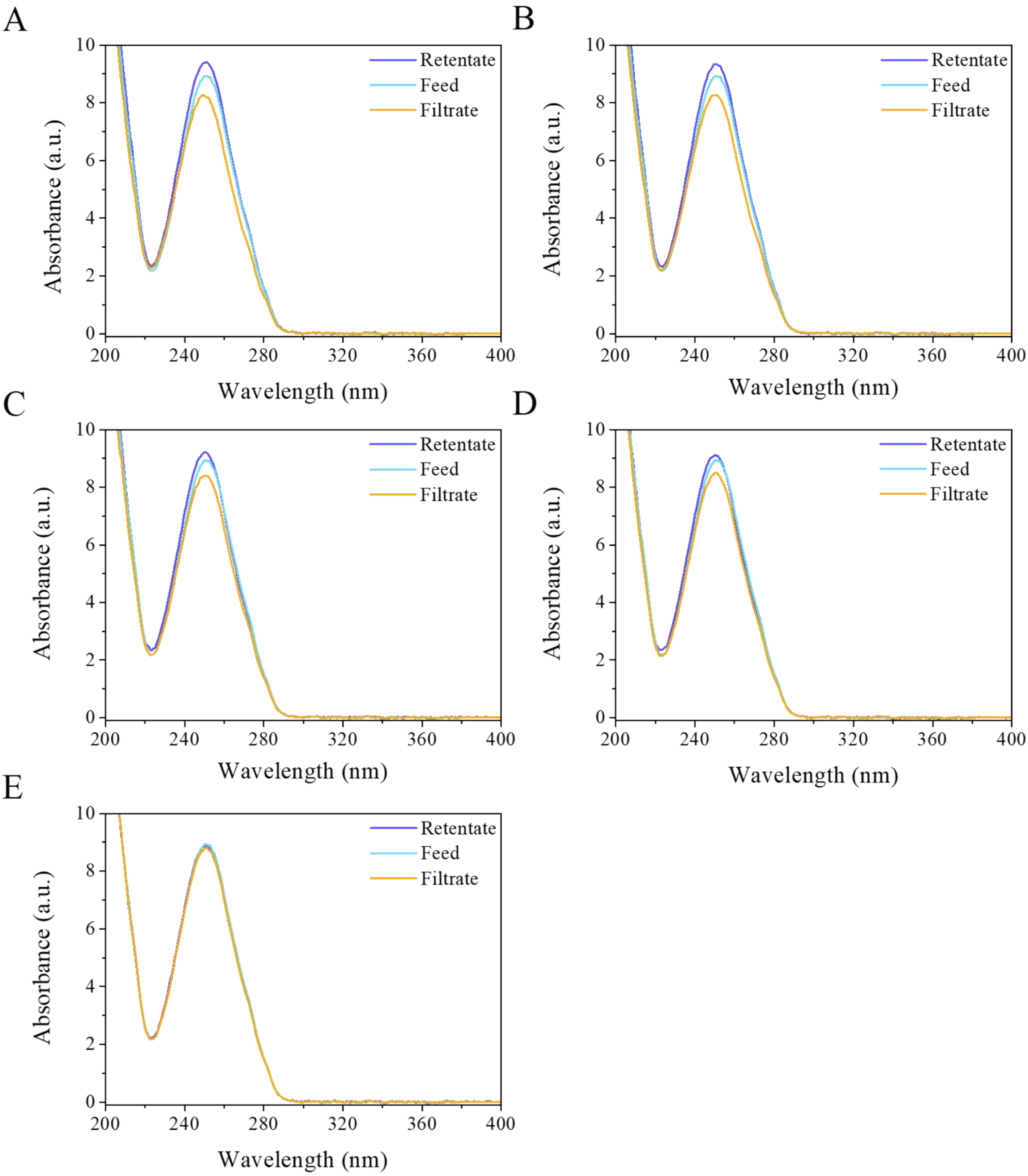

Figure S20. Determination of MO's concentration in feed, filtrate and retentate, after half of the solution permeated through the membrane. (A) Spectrum of solutions using GOM as the testing membrane. (B) Spectrum of solutions using SGM-0.01 as the testing membrane. (C) Spectrum of solutions using SGM-0.1 as the testing membrane. (D) Spectrum of solutions using SGM-1 as the testing membrane. (E) Spectrum of solutions using SGM-10 as the testing membrane.

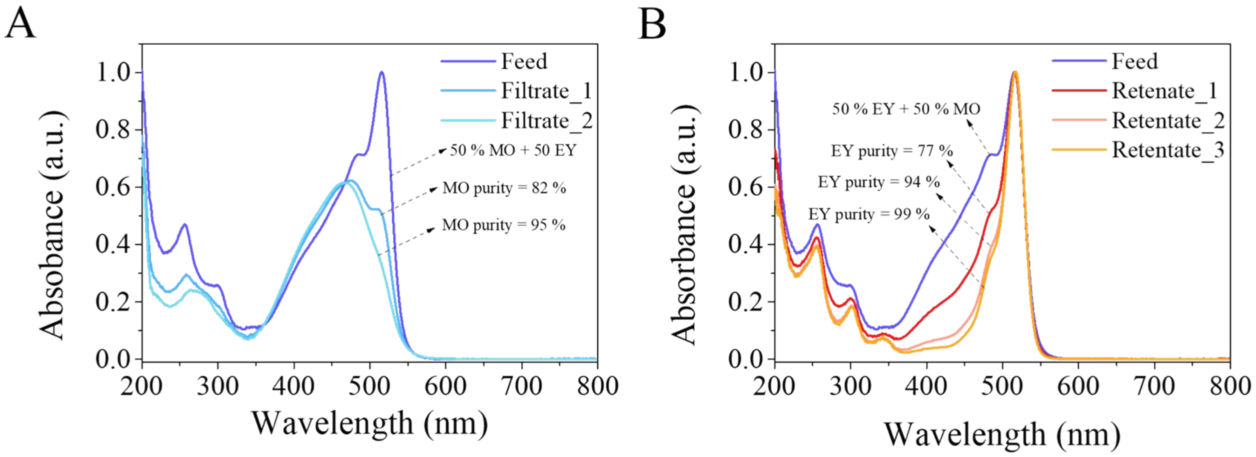

Figure S21. Separation of mixed EY and MO by filtrating the mixture through SGM-1. (A) UV spectra of mixed EY + MO solution and the filtrate after one time and two times filtration. (B) UV spectra of mixed MO + EY solution and the retentate after one time, two times and three times filtration.

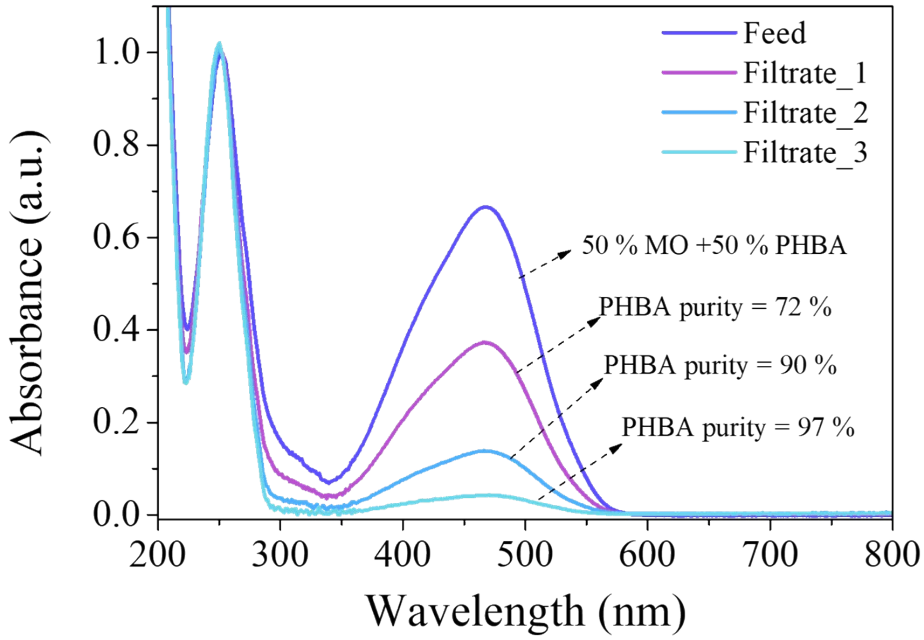

Figure S22. UV spectra of filtrate after each time's purification.

Table S2. Operation condition and flux during similar molecule separation

Mixture	Membrane	Operation pressure(Bar)	Flux (L/m^2/h)
EY + PHBA	SGM-1	1	~ 7.2
EY + MO	SGM-1	1	~ 7.5
MO + PHBA	SGM-0.1	1	~ 5.4